

The Characterization and Mercury Oxidation Performance of Bromine-Doped Vanadia/Titania Oxide Catalyst

Yuntao Li^{1*}, Gong Chen¹, Xuanxiong Kang¹, Linzhi Zhai^{2*}, Shuling Dong³, Mengjun Huang¹, Hongpan Liu¹

¹Chongqing Key Laboratory of Environmental Materials and Remediation Technologies, College of Chemistry & Environmental Engineering (Chongqing University of Arts and Sciences), Chongqing, PR China

²School of Environmental and Chemical Engineering, Jiangsu University of Science and Technology, Zhenjiang, PR China

³School of Chemistry, Biology and Materials Engineering, Suzhou University of Science and Technology, Suzhou, PR China

*Corresponding author:

Yuntao Li

Chongqing Key Laboratory of Environmental Materials and Remediation Technologies, College of Chemistry & Environmental Engineering (Chongqing University of Arts and Sciences), Chongqing 402160, PR China.

Linzhi Zhai

School of Environmental and Chemical Engineering, Jiangsu University of Science and Technology, Zhenjiang 212000, PR China.

Received : November 10, 2019

Published : November 26, 2019

INTRODUCTION

Mercury and its compounds have considerable harm to the human digestive system, central nervous system and kidneys, and are one of the persistent environmental pollutants that are currently receiving sustained attention. One of the main sources of mercury in the atmosphere is coal-fired emissions. On January 19, 2013, the United Nations Environment Program adopted the Minamata Convention, an international convention for the control and reduction of mercury emissions worldwide. The Convention requires the control of mercury emissions from various large coal-fired power station boilers and industrial boilers. Therefore, mercury emission control

ABSTRACT

Mercury pollution produced by coal combustion has been identified as a severe hazardous pollutant to human health and the environment. For the coal-fired power plants, one of the most cost-effective methods to control mercury is to use SCR catalysts, which can achieve both denitration and oxidation effects, simultaneously. In the present study, a new SCR catalyst, bromine-doped vanadia/titania oxide, has been developed, and its structure and mercury oxidation characteristics were systematically studied. Results demonstrated that, in compare to the control sample, bromine-doped vanadia/titania oxide has obviously higher amount of V⁴⁺ and Ti³⁺, thus resulting in an improved redox property. Activity tests showed that the catalytic capacity was highly dependent on the doping amount of bromine with a specific feature from 'low to high to low'. The highest value for mercury oxidation of the product is [Br]/[Ti]=1.2×10⁻².

Keywords: Minamata Convention, mercury control, SCR denitration catalyst, bromine doping.

of coal combustion is one of the hot spots of environmental protection research.

Mercury control methods in coal-fired power plants can be divided into mercury removal before combustion (pre-stage technology), mercury removal during combustion, and mercury removal after combustion (back-end technology). Among them, the widely used technologies include bromine-treated coal before combustion and injecting brominated activated carbon into the flue gas after combustion, these two technologies have been industrially applied abroad, but the investment and operating costs are high [1]. On the other hand, coal-fired power plants in China are basically equipped with

selective catalytic reduction (SCR) denitration equipments, electrostatic precipitators and wet desulfurization facilities, and a large number of field test results [2] show that the combined use of SCR, electrostatic precipitator and wet desulfurization facilities could effectively reduce gaseous mercury emissions. The author has also tested three power plants in China and found that the mercury removal efficiency of the electrostatic precipitator system is 7.85%~44.63%, and the mercury removal efficiency of the wet desulfurization system is 43.63%~75.35% (the mercury was basically all present in the gypsum). Less than 20% of the mercury was emitted and was mainly elemental mercury. These test results fully demonstrate that the use of installed SCR, electrostatic precipitator and wet desulfurization facilities to achieve synergistic mercury removal is an effective and low-cost mercury removal technology.

The key to achieving synergistic mercury removal by SCR, electrostatic precipitator and wet desulfurization facilities is to develop a SCR catalyst with high elemental mercury oxidation rate. Existing commercial SCR catalysts have been proven over the long term and improvements based on existing commercial SCR catalysts will significantly reduce the difficulty of mercury control engineering applications. When testing the commercial $V_2O_5-WO_3/TiO_2$ honeycomb SCR catalyst, the authors found that although the catalyst has a good deNO_x effect, the oxidation rate of mercury was less than 10% (test conditions are based on the VGB test standard). The results of Schwämmle et al. [3] has shown that increasing the wall thickness of the honeycomb catalyst could increase the mercury oxidation capacity of commercial SCR catalysts. But this is equivalent to increasing the amount of catalyst, which leads to an increase in SO₂ conversion. So, how should the mercury oxidation performance of existing commercial SCR catalysts be improved?

The mechanism of oxidation of elemental mercury on the surface of SCR catalysts yielded different results under different catalysts and different test conditions, Eley–Rideal mechanism [4], Langmuir–Hinshelwood mechanism [5-8] and Mars–Maessen mechanism [9,10] were possible. The oxidation of elemental mercury on the surface of the SCR catalyst is a heterogeneous catalytic reaction process. Regardless of the reaction mechanism, the adsorption of the reactants and the redox capability of the catalyst are core. Theoretical results showed that on the surface of oxygen defects, the adsorption energy of Hg⁰ was much higher than that on the clean surface, which was a strong chemical adsorption; while the doping caused the incompletely coordinated O atoms to

have strong adsorption to Hg. The presence of surface active oxygen species plays an important role in the adsorption of mercury [10, 11]. The mercury oxidation process promoted the conversion of V⁵⁺ species into V⁴⁺ species and consumed lattice oxygen on the catalyst surface [12]. The transfer efficiency of electrons between V⁵⁺, V⁴⁺ and other catalyst components such as vanadium and titanium has an important influence on the mercury oxidation reaction. Therefore, we can further study the SCR catalysts with high elemental mercury oxidation rate from the promotion of the adsorption of elemental mercury by SCR catalysts and the redox capacity of SCR catalysts.

At present, the main idea in the study of SCR catalysts for elemental mercury oxidation is to add different transition metal oxides or combinations thereof [13], such as Co-Mn [10], CeO₂ [14,15], Mo-Ru [16], RuO₂ modified Ce-Zr complex [17], Au/TiO₂ [18], CuCl₂/γ-Al₂O₃ [19], Graphene enhanced Mn-Ce binary metal oxides [20], Fe₂O₃ [21,22], CuCl₂-CoOx/Ti-CeOx [23], Co-MF [24], manganese oxide octahedral molecular sieve [25], Mn-Fe co-modified ZSM-5 [26], etc. These studies are important in how to promote the adsorption of the catalyst on elemental mercury and improve the redox capacity of the catalyst. However, is there any other way to strengthen the mercury oxidation capacity of the SCR catalyst? Existing mature mercury removal technology, coal treated by bromine can promote the oxidation of elemental mercury in the combustion process, brominated activated carbon can enhance the adsorption and oxidation of elemental mercury and brominated activated carbon is better than chlorinated activated carbon, HBr in the flue gas is better than HCl for mercury oxidation [27], which showed the importance of non-metallic bromine in mercury control. In view of this, this paper studies the effect of non-metallic bromine doping on the structure and performances of vanadia/titania catalyst from a non-metallic perspective, exploring new ideas for elemental mercury oxidation by SCR catalysts.

EXPERIMENTAL

Preparation of Br-doped V/TiO₂

The bromine-doped carrier titanium oxide was first prepared by the sol-gel method, and then vanadium oxide was impregnated. Typical experiment, as follows: First, 21.7830 g (0.064 mol) of butyl titanate (C₁₆H₃₆O₄Ti) was added into 0.128 mol of acetylacetone (acacH, C₆H₈O₂) solution, keeping the molar ration of [acacH]/[Ti]=2. Then, 50 mL ammonium bromide (NH₄Br)/ethanol mixed solution was poured to above C₁₆H₃₆O₄Ti/ C₆H₈O₂ solution, stirring for 2 hours to form a sol.

Thereafter, the sol product was heated at 333 K, followed by evaporating for 6 h at 393 K. The resultant product was calcined at 773K for 3 h, the Br-doped TiO_2 powder was obtained. Finally, the Br-doped TiO_2 powder (particle size was 0.70-0.90mm) was immersed in NH_4VO_3 aqueous solution, refluxing for 4 h at 333 K, and dried for 6 h at 393 K, sequently. The powder was calcined at 623 K for 4 h to obtain a Br-doped V/ TiO_2 catalyst. The catalyst sample is designated as VTiBr x, (where x represents $100 \times [\text{Br}]/[\text{Ti}]$, $[\text{Br}]/[\text{Ti}] = 0 \sim 2 \times 10^{-2}$).

Characterization of Br-doped V/ TiO_2

The X-ray photoelectron spectroscopy (XPS) was performed by the ESCALAB 250Xi device of ThermoFisher Scientific. The X-ray diffraction spectrum (XRD) was tested by the D8 X-ray diffractometer of Bruker. The specific surface area and pore structure were determined by the ASAP2460 of Micromeritics. The electronic paramagnetic resonance (EPR) spectrum of the sample was detected by the A300 equipment of Bruker. The elemental composition of the sample is quantitatively analyzed by Agilent's Agilent 725 series ICP-OES equipment. The Photoluminescence spectrum (PL) was tested by the FLs980 full-function steady-state/transient fluorescence spectrometer from Edinburgh Instruments.

Mercury oxidation performance test

The mercury oxidation performance test was carried out in a fixed-bed reactor (inner diameter 6.8 mm). The experimental scheme was shown in (Figure 1). 0.3 g catalyst was filled, then the simulated flue gas ($3 \times 10^{-5} \mu\text{g}/\text{mL}$ Hg + 5% O_2 , and the rest was N_2 flow) was passed at 150 mL/min. The Hg was placed into a quartz U-tube with a mercury permeation tube (VICI Metronics, USA) embedded in an isothermal water bath, then mercury vapor was provided into the gas stream through N_2 current.

Before the mercury oxidation performance test, the simulated flue gas was introduced into the fixed-bed reactor for 48 h to ensure the Hg-adsorption saturation by the Br-doped V/ TiO_2 . The set temperature was stable for more than 1h, and the concentration of Hg was analyzed by the coal-fired flue gas mercury analyzer QM201H.

Hg conversion (X) is defined as:

$$X = (\text{Hg}_{\text{in}} - \text{Hg}_{\text{out}}) / \text{Hg}_{\text{in}} \quad (1)$$

The reaction kinetic order for Hg^0 in the SCR catalyst oxidation, elemental mercury reaction was one [28], and the reaction

kinetic order of O_2 was zero. Thus, the reaction rate of oxidizing Hg^0 is:

$$r = kC_{\text{Hg}^0}^0 \quad (2)$$

In order to compare the activity of different vanadia-based catalysts, the rate constant k_m was used as an evaluation index:

$$k_m = -\frac{F_{\text{Hg}}^0}{w_m P_{\text{Hg}}^0} \ln(1 - X) \quad (3)$$

Where P_{Hg}^0 was the partial pressure of Hg^0 ; F_{Hg}^0 was the molar flow of Hg^0 at the inlet of the reactor; w_m is the mass of vanadium [29].

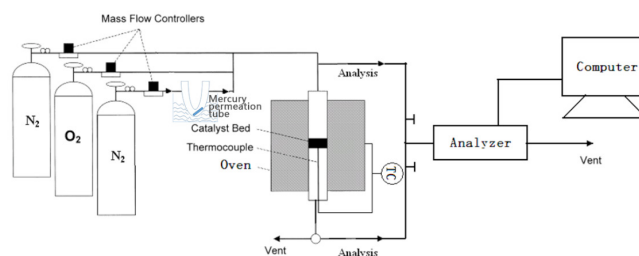


Figure 1: Mercury oxidation performance test experimental procedure.

RESULTS AND DISCUSSION

Pore structure and composition analysis

The vanadia content was detected by ICP analysis (Table 1). The results indicated that the active vanadia content of the Br-doped V/ TiO_2 was 0.60~0.75%, which was lower than some conventional V-based SCR catalysts. The surface vanadium density (n_s) was small, and the active component was in an effective dispersion state.

It was found that the vanadia content of commercial SCR catalysts used in China was generally 0.3~1.5% to ensure the high deNOx efficiency, small SO_2 oxidation and ammonia slip. Therefore, the preparation of SCR catalysts with lower vanadium content and high mercury oxidation efficiency still has large challenges.

^aObtained by the formula $n_s = \text{V}_2\text{O}_5 \% \times 6.02 \times 10^{23} \times 2 / (S_{\text{BET}} \times 182 \times 10^{18})$ [30].

According to the physical adsorption isotherm classification proposed by IUPAC [31], the hypothermic N_2 adsorption isotherms of the Br-doped V/ TiO_2 showed hysteresis loops, and capillary agglomeration occurred, which belonged to type IV isotherms (Figure 2). This isotherm was produced

by mesopores, which consistent with the measured average pore diameter (between 7 and 17 nm). From the hysteresis loops, the change of the adsorption amount was not very steep but rather slow, indicating that the pore distribution range was relatively wide, and it should be a mixture of the cylindrical hole with open ends and the slit hole with parallel plate structure. When the relative pressure (P/P_0) was low, the gas diffuses in the pores with a pore diameter of 1.5~100 nm, which is generally Knudsen diffusion

Table 1: Vanadia content, BET specific area, n_s and the kinetic constants of the catalysts.

	V_2O_5	S_{BET}	n_s	$k_m(593K)$	$k_m(623K)$
	(%wt)	($m^2 g^{-1}$)	($VO_x nm^{-2}$) ^a	($mol Hg(g V)^{-1} Pa^{-1} s^{-1}$)	($mol Hg(g V)^{-1} Pa^{-1} s^{-1}$)
VTiBr 0	0.62	20.41	2.01	2.52×10^{-6}	1.71×10^{-6}
VTiBr 0.4	0.6	24.99	1.59	3.93×10^{-6}	3.11×10^{-6}
VTiBr 0.8	0.75	22.12	2.24	4.67×10^{-6}	3.38×10^{-6}
VTiBr 1.2	0.69	21.59	2.11	9.91×10^{-6}	6.76×10^{-6}
VTiBr 1.6	0.63	25.99	1.6	7.61×10^{-6}	5.23×10^{-6}
VTiBr 2	0.69	27.44	1.66	5.38×10^{-6}	3.55×10^{-6}

In this study, N_2 , O_2 and Hg were diffused in the Br-doped V/TiO₂ catalyst by Knudsen diffusion. The resistance comes from the collision of molecules with the pore walls, and the diffusion coefficient D_k mainly depends on the temperature T and the pore radius r .

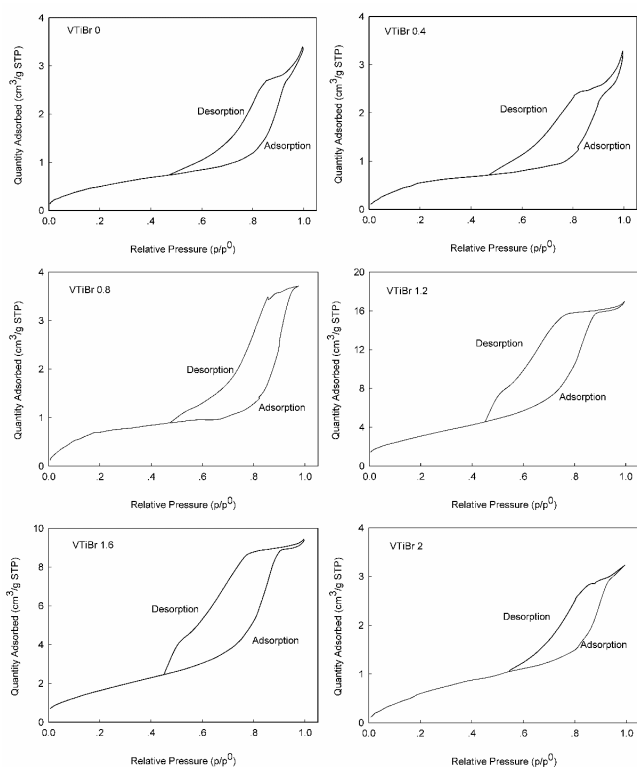


Figure 2: N_2 adsorption-desorption curves of catalysts.

Crystal Structure Analysis

The XRD data was obtained in **Figure 3**. The diffraction peak of the anatase phase TiO₂ (JCPDS 21-1272) in the bromine-doped catalyst were narrower and stronger than that of the undoped Br sample (VTiBr0). Br may promote the formation of the crystal. In addition, compared with VTiBr 0, the diffraction angle of the anatase phase TiO₂ on the Br-doped V/TiO₂ becomes smaller, and the interplanar spacing of the crystal increases. According to the Bragg diffraction formula, this indicates that a solid solution is formed on the Br-doped catalyst.

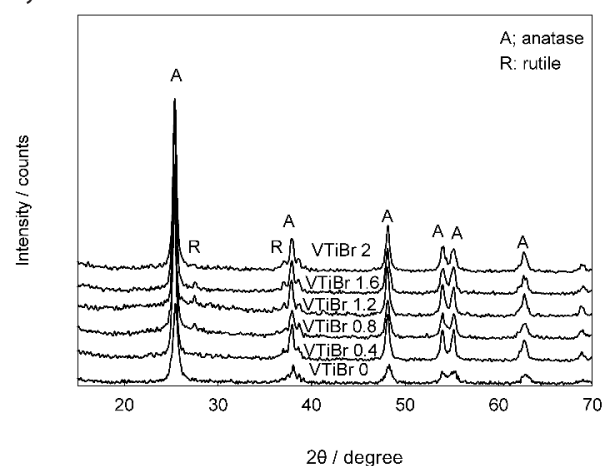


Figure 3: XRD analysis results of catalysts.

Element valence analysis

Figure 4 showed the EPR spectrum of the Br-doped V/TiO₂ products at room temperature, which manifested an amount of V⁴⁺ ions grew on its surface and bulk phase. Although the loading of vanadia was low (**Table 1**), peaks belonging to V⁴⁺ ions can be clearly detected. By integrating the peaks of V⁴⁺ ions, the peak area reduced in the following order: VTiBr 1.2 > VTiBr 1.6 > VTiBr 0.8 > VTiBr 2 > VTiBr 0.4 > VTiBr 0. With the increasing of the Br-doping, the generated V⁴⁺ ions VTiBr 1.2 were the most among the Br-doped V/TiO₂ samples.

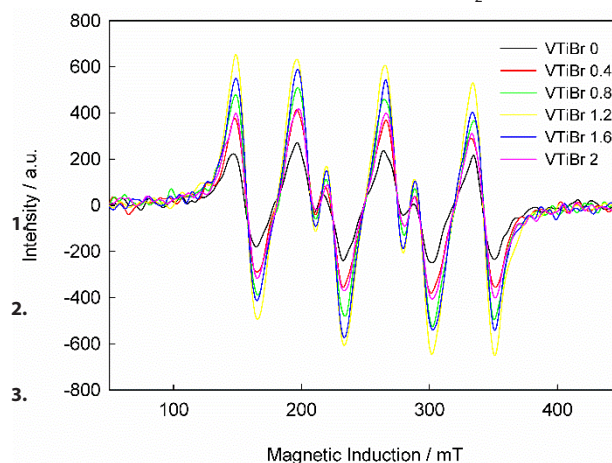


Figure 4: EPR spectra of different Br-doped content catalysts.

Figure 5 showed the XPS spectra of the samples. As can be seen from **Figure 5d**, after the bromine was doped, the peaks shifted toward the low binding energy direction. **Figure 5** showed that the Ti 2p_{3/2}, V 2p_{3/2} and O 1s peaks of VTiBr 1.2 were shifted by about 0.2 eV, 0.5 eV and 0.3 eV, respectively, in the direction of low binding energy compared to the sample VTiBr 0. This meant that the electrons was lost on Ti and V, and the electrons obtained by O, so, the valence states of Ti and V were not completely +4 and +5, respectively. In addition, since the amount of doping of bromine was small, no significant Br information was obtained in **Figure 5d**.

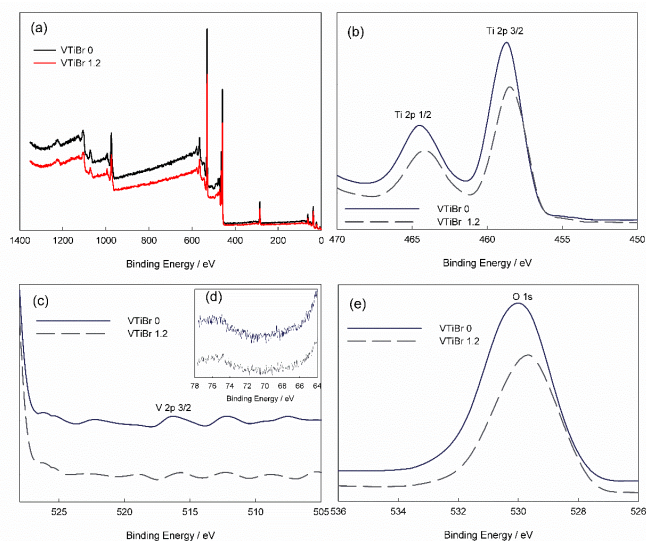


Figure 5: XPS spectra of the catalysts.

PL spectral analysis

In order to further discuss the effect of bromine on the structure of the catalyst, the photoluminescence properties of the samples were studied. In general, the emission peak of anatase TiO₂ is about 380 nm. It can be seen from **Figure 6** that after the introduction of bromine, the emission peak at about 380 nm moved toward the long wavelength direction, which showed the molecular rigidity increased. The emission peak at about 376 nm moved to the short wavelength direction, and the emission peak at around 376 nm was enhanced after the addition of bromine. Typically, electron withdrawing groups weaken or even quench fluorescence. Oxygen has a higher electron absorption capacity than bromine, and fluorescence should be enhanced after bromine doping [32]. Therefore, the emission peak at around 376 nm should be related to the electron-withdrawing group oxygen and bromine.

The peak at 530 nm in **Figure 7** indicated the presence of a color center with one electron [33-37], which was still present but reduced after bromine doping. Since oxygen adsorption to the color center can reduce the luminescence

properties of the sample [38], the luminescence peak of the bromine-doped sample at 530 nm was weaker than that of the undoped sample, indicating the difference in oxygen adsorption capacity between the two samples, that is, the bromine-doped sample can adsorb more oxygen than the undoped sample.

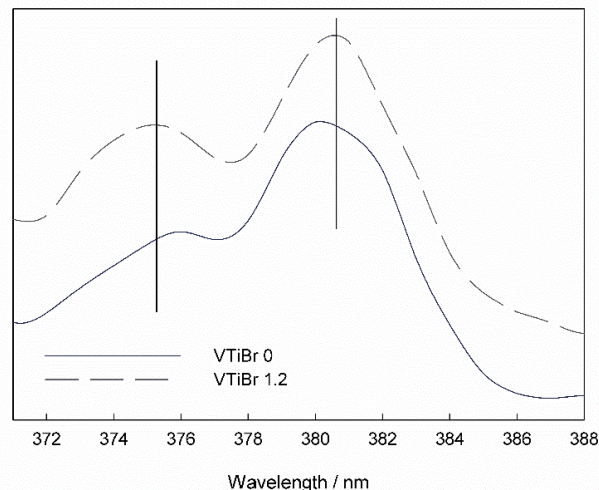


Figure 6: PL spectra of the catalysts.

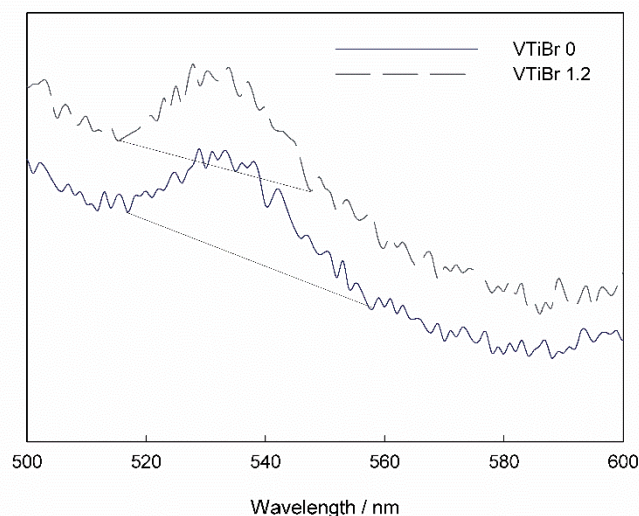


Figure 7: PL spectra around 530 nm of the catalysts.

From the characterization results of EPR, XPS and PL, it can be seen that the samples in this study contained mixed valences of Ti and V, and bromine doping could increase the amount of V⁴⁺ and Ti³⁺, that is, the reduction characteristics or redox characteristics of the catalysts after bromine doping were improved [39-42].

Elemental mercury oxidation performance

In order to evaluate the effect of bromine doping on the mercury oxidation performance, the elemental mercury oxidation activity of the catalyst was tested with the simulated flue gas. The results (**Table 1** and **Figure 8**) showed that

bromine could significantly improve the mercury oxidation performance. As the bromine doping amount increased, the activity first increased and then decreased, and the VTiBr 1.2 sample has the highest mercury oxidation efficiency. In addition, the mercury oxidation performance decreased with temperature increasing, possibly the high temperature may inhibit the adsorption of mercury on the samples.

In the mercury oxidation performance test, there was no hydrogen halide involved such as HCl, thus, it is no longer necessary to spray hydrogen halide into the flue gas under the actual application condition, which avoided the corrosion of hydrogen halides on the equipment, thus also reduced the operating costs. The test results also validated our catalyst design ideas.

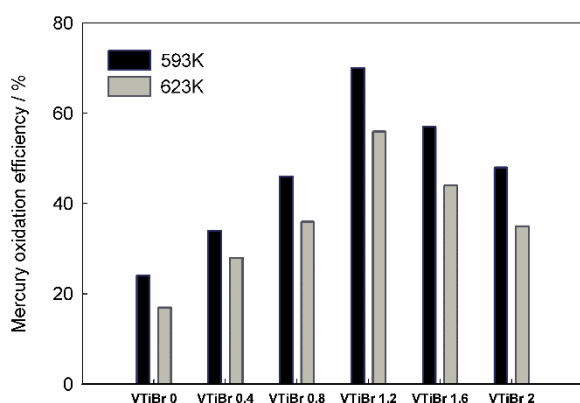


Figure 8: Activity test results of elemental mercury oxidation.

Testing conditions: the simulated flue gas flow rate was 150 ml/min, and its composition was 3×10^{-5} $\mu\text{g/ml}$ Hg + 5% O_2 , and the rest was N_2 . Catalyst usage 0.3 g.

CONCLUSIONS

In order to reduce the mercury control cost of coal-fired flue gas, it is an effective and feasible way to control mercury by SCR denitrification synergistic oxidation. By analyzing the importance of non-metallic bromine in the existing mature mercury removal technology, this paper studied the effect of non-metallic bromine doping on the structure and properties of vanadia/titania catalyst from a non-metallic perspective, exploring new ideas for elemental mercury oxidation by SCR catalysts. The results showed that after bromine doping, the samples in this study contained mixed valences of Ti and V, and the bromine doping could increase the amount of V^{4+} and Ti^{3+} , that is, the reduction characteristics or redox characteristics of the catalysts after bromine doping were improved. According to the basic theory of gas-solid phase catalytic reaction, the

increase of the redox capacity of the catalyst enhances the catalytic activity of the catalyst, which was verified in the activity test. As the bromine doping amount increased, the activity first increased and then decreased, and the VTiBr 1.2 sample has the highest mercury oxidation performance.

Acknowledgements

The authors want to thank the financial support from the Scientific and Technological Research Program of the Chongqing Municipal Education Commission (KJ1711266/ KJ1711286/ KJ1711290) and the Research Program of Chongqing University of Arts and Sciences (No: R2016CH07/ No: 2017RCH07). We gratefully acknowledge the many important contributions from the researchers of all the reports cited in this paper.

REFERENCES

1. Heidel B, Rogge T, Scheffknecht G (2016) Controlled desorption of mercury in wet FGD waste water treatment. *Appl Energy* 162: 1211-1217.
2. Lee C, Serre S, Zhao Y, Lee SJ, Hastings TW (2006) Study of the effect of chlorine addition on mercury oxidation by SCR catalyst under simulated subbituminous coal flue gas. In Proceedings, EPA-DOE-EPRI-A&WMA Power Plant Air Pollutant Control "Mega" Symposium, Baltimore, MD, USA [Internet].
3. Schwammlea T, Bertschea F, Hartungb A, Brandensteinc J, Heidela B, Scheffknechta G (2013) Influence of geometrical parameters of honeycomb commercial SCR-DeNOx-catalysts on DeNOx-activity, mercury oxidation and SO_2/SO_3 -conversion. *Chem Eng J* 222: 274-281.
4. Wang Z, Liu J, Zhang B, Yang Y, Zhang Z, Miao S (2016) Mechanism of heterogeneous mercury oxidation by HBr over $\text{V}_2\text{O}_5/\text{TiO}_2$ catalyst. *Environ Sci Technol* 50 (10): 5398-5404.
5. Zhang B, Liu J, Yang Y, Chang M (2015) Oxidation mechanism of elemental mercury by HCl over MnO_2 catalyst: Insights from first principles. *Chem Eng J* 280: 354-362.
6. Zhao B, Liu X, Zhou Z, Shao H, Xu M (2016) Catalytic oxidation of elemental mercury by Mn-Mo/CNT at low temperature. *Chem Eng J* 284: 1233-1241.

7. Zhao S, Li Z, Qu Z, Yan N, Huang W, Chen W, et al. (2015) Co-benefit of Ag and Mo for the catalytic oxidation of elemental mercury. *Fuel* 158: 891-897.
8. Zhou Z, Liu X, Zhao B, Shao H, Xu Y, Xu (2016). M Elemental mercury oxidation over manganese-based perovskite-type catalyst at low temperature. *Chem Eng J* 288: 701-710.
9. Zhao L, Li C, Zhang J, Zhang X, Zhan F, Ma J, et al. (2015) Promotional effect of CeO₂ modified support on V₂O₅-WO₃/TiO₂ catalyst for elemental mercury oxidation in simulated coal-fired flue gas. *Fuel* 153: 361-369.
10. Zhang A, Zheng W, Song J, Hu S, Liu Z, Xiang J (2014) Cobalt manganese oxides modified titania catalysts for oxidation of elemental mercury at low flue gas temperature. *Chem Eng J* 236: 29-38.
11. Ling L, Zhao Z, Zhao S, Wang Q, Wang B, Zhang R, et al. (2017) Effects of metals doping on the removal of Hg and H₂S over ceria. *Appl Surf Sci* 403: 500-508.
12. Yang J, Yang Q, Sun J, Liu Q, Zhao D, Gao W, et al. (2015) Effects of mercury oxidation on V₂O₅-WO₃/TiO₂ catalyst properties in NH₃-SCR process. *Catal Commun* 59: 78-82.
13. Zhao L, Li C, Zhang X, Zeng G, Zhang J, Xie Y (2015) A review on oxidation of elemental mercury from coal-fired flue gas with selective catalytic reduction catalysts. *Catal Sci Technol* 5: 3459-3472.
14. Yang Y, Liu J, Zhang B, Zhao Y, Chen X, Shen F (2017) Experimental and theoretical studies of mercury oxidation over CeO₂ - WO₃/TiO₂ catalysts in coal-fired flue gas. *Chem Eng J* 317: 758-765.
15. Jampaiah D, Tur K M, Venkataswamy P, Ippolito S J, Sabri Y M, Tardio J, et al. (2015) Catalytic oxidation and adsorption of elemental mercury over nanostructured CeO₂-MnOx catalyst. *RSC Advances* 5(38): 30331-30341.
16. Chen W, Ma Y, Yan N, Qu Z, Yang S, Xie J, et al. (2014) The co-benefit of elemental mercury oxidation and slip ammonia abatement with SCR-Plus catalysts. *Fuel* 133: 263-269.
17. Songjian Zhao, Wanmiao Chen, Wenjun Huang, Jiangkun Xie, Zan Qu, Naiqiang Yan (2018) Elemental mercury catalytic oxidation removal and SeO₂ poisoning investigation over RuO₂ modified Ce-Zr complex. *Appl Catal A Gen* 564: 64-71.
18. Dranga B, Koeser H (2015) Increased co-oxidation activity for mercury under hot and cold site coal power plant conditions – Preparation and evaluation of Au/TiO₂-coated SCR-DeNOx catalysts. *Appl Catal B* 166-167: 302-312.
19. Liu Z, Li X, Lee J-Y, Bolin T B (2015) Oxidation of elemental mercury vapor over γ-Al₂O₃ supported CuCl₂ catalyst for mercury emissions control. *Chem Eng J* 275: 1-7.
20. Yongpeng Ma, Bailong Mu, Xiaojing Zhang, Dongli Yuan, Chuang Ma, Haomiao Xu, et al. (2019) Graphene enhanced Mn-Ce binary metal oxides for catalytic oxidation and adsorption of elemental mercury from coal-fired flue gas, *Chem Eng J* 358: 1499-1506.
21. Yang Y, Liu J, Wang Z, Liu F (2017) Heterogeneous reaction kinetics of mercury oxidation by HCl over Fe₂O₃ surface. *Fuel Process Technol* 159: 266-271.
22. Huang W, Xu H, Qu Z, Zhao S, Chen W, Yan N (2016) Significance of Fe₂O₃ modified SCR catalyst for gas-phase elemental mercury oxidation in coal-fired flue gas. *Fuel Process Technol* 149: 23-28.
23. Li H, Wang S, Wang X, Hu J (2017) Activity of CuCl₂-modified cobalt catalyst supported on Ti-Ce composite for simultaneous catalytic oxidation of Hg⁰ and NO in a simulated pre-sco process. *Chem Eng J* 316: 1103-1113.
24. Yang J, Zhao Y, Chang L, Zhang J, Zheng C (2015) Mercury adsorption and oxidation over cobalt oxide loaded magnetospheres catalyst from fly ash in oxyfuel combustion flue gas. *Environ Sci Technol* 49 (13): 8210-8218.
25. Xi Liu, Shaojian Jiang, Hailong Li, Jianping Yang, Zequn Yang, Jiexia Zhao, et al. (2019) Elemental mercury oxidation over manganese oxide octahedral molecular sieve catalyst at low flue gas temperature. *Chem Eng J* 356: 142-150.
26. Zhen Zhang, Jiang Wu, Bin Li, Huibin Xu, Dongjing Liu (2019) Removal of elemental mercury from simulated flue gas by ZSM-5 modified with Mn-Fe mixed oxides. *Chem Eng J* 375: 121946.
27. Stollea R, Koesera Heinz, Heinz Gutberlet (2014) Oxidation and reduction of mercury by SCR DeNOx catalysts under flue gas conditions in coal fired power plants. *Appl Catal B* 144: 486-497.

28. Lingkui Zhao, Caiting Li, Xunan Zhang, Guangming Zeng, Jie Zhang, Yin'e Xie (2015) A review on oxidation of elemental mercury from coal-fired flue gas with selective catalytic reduction catalysts, *Catal Sci Technol* 5(7): 3459-3472.
29. Valdés-Solís T, Marbán G, Fuertes A B (2003) Low-temperature SCR of NO_x with NH₃ over carbon-ceramic supported catalysts. *Appl Catal B* 46(2): 261-271.
30. Chen K, Xie S, Iglesia E, Bell A T (2000) Structure and properties of zirconia-supported molybdenum oxide catalysts for oxidative dehydrogenation of Propane. *J Catal* 189(2): 421-430.
31. Matthias Thommes, Katsumi Kaneko, Alexander V. Neimark, James P. Olivier, Francisco Rodriguez-Reinoso, Jean Rouquerol, et al. (2015). Physisorption of gases, with special reference to the evaluation of surface area and pore size distribution (IUPAC Technical Report), *Pure appl Chem* 87(9-10): 1051-1069.
32. Notestein, JM, Iglesia E, Katz A (2007) Photoluminescence and Charge-Transfer Complexes of Calixarenes Grafted on TiO₂ Nanoparticles, *Chem Mater* 19(20): 4998-5005.
33. Li D, Haneda H, Hishita S, Ohashi N, Labhsetwar N K (2005) Fluorine-doped TiO₂ powders prepared by spray pyrolysis and their improved photocatalytic activity for decomposition of gas-phase acetaldehyde *J Fluor Chem*. 126(1): 69-77.
34. Li D, Haneda H, Labhsetwar N K, Hishita S, Ohashi N (2005) Visible-light-driven photocatalysis on fluorine-doped TiO₂ powders by the creation of surface oxygen vacancies. *Chem Phys Lett* 401(4-6): 579-584.
35. Li D, Ohashi N, Hishita S, Kolodiaznyhny T, Haneda H (2005) Origin of visible-light-driven photocatalysis: A comparative study on N/F-doped and N-F-codoped TiO₂ powders by means of experimental characterizations and theoretical calculations. *J Solid State Chem* 178(11): 3293-3302.
36. Lei Y, Zhang L D, Meng G W, Li G H, Zhang X Y, Liang C H, et al. (2001) Preparation and photoluminescence of highly ordered TiO₂ nanowire arrays. *Appl Phys Lett* 78(8): 1125-1127.
37. Rui Zhang, Qin Zhong, Wei Zhao, Lemeng Yu, Hongxia Qu (2014) Promotional effect of fluorine on the selective catalytic reduction of NO with NH₃ over CeO₂-TiO₂ catalyst at low temperature. *Appl Surf Sci* 289: 237-244.
38. Anpo M, Che M, Fubini B, Garrone E, Giamello E, Paganini M C (1999) Generation of superoxide ions at oxide surfaces. *Top Catal* 8(3-4): 189-198.
39. Narayana K V, Raju B D, Masthan S K, Rao V V, Rao P K, Subrahmanian R, et al. (2004) ESR spectroscopic characterization of V₂O₅/AlF₃ ammoxidation catalysts. *Catal Commun* 5(8): 457-462.
40. Scheurell K, Kemnitz E (2005) Amorphous aluminium fluoride as new matrix for vanadium-containing catalysts. *J Mater Chem* 15(45): 4845-4853.
41. Scheurell K, Scholz G, Kemnitz E (2007) Structural study of VO_x doped aluminium fluoride and aluminium oxide catalysts. *J Solid State Chem* 180(2): 749-758.
42. Scheurell K, Scholz G, Pawlik A, Kemnitz E (2008) VO_x doped Al₂O₃ and AlF₃ -a comparison of bulk, surface and catalytic properties. *Solid State Sci* 10(7): 873-883.